A BLIND ALGORITHM BASED ON DIFFERENCE OF NORMS FOR EQUALIZATION OF BIORTHOGONAL SIGNALS

A.G. Klein, C.R. Johnson, Jr.[*]

Cornell University
School of Electrical & Computer Engineering
Ithaca, NY 14853, USA

P. Duhamel

Supélec/LSS
3, rue Joliot-Curie
91192 Gif-sur-Yvette, FRANCE

ABSTRACT

Motivated by increasing interest in energy efficient modulations, we investigate a blind algorithm for biorthogonal signaling. While this modulation has historically been considered only for use in narrowband systems without intersymbol interference (ISI), recent attention has been given to its use in ISI channels. Due to the fact that biorthogonal modulation (BOM) results in a source that is not i.i.d., however, classical adaptive equalization techniques cannot be directly applied to equalization of BOM signals. We review the MMSE and LMS-based equalizers, and then identify some peculiarities that arise in blind equalization of BOM signals when compared to more traditional modulations like BPSK. Next, we present a novel blind algorithm, called TROMBONE, for the adaptive equalization of BOM signals. We discuss the convergence properties of this algorithm, and demonstrate its performance with numerical simulations.

1. INTRODUCTION

Increasing amounts of available unregulated spectrum, combined with an increasing demand for battery-operated wireless devices has spurred an interest in modulation schemes that give up some bandwidth efficiency in exchange for energy efficiency. Biorthogonal modulation (BOM) or M-ary biorthogonal keying (MBOK) is one such modulation scheme that has recently been considered for use in several consumer wireless standards. In the WLAN and WPAN applications where BOM has been considered, it is well-known that intersymbol interference (ISI) will be present, and ISI is viewed to be a serious impairment to acceptable performance. While the optimum detector in ISI is the maximum likelihood sequence estimator (MLSE), its complexity is usually too high for practical implementation, and thus suboptimal schemes are desirable. Several very recent works have addressed this issue, notably [1] and [2]. In [1], a blind algorithm was developed for BOM based on a dispersion minimization criterion. Non-adaptive ISI compensation for BOM signals was considered in [2], wherein the authors conduct a simulation study of a reduced state Viterbi equalizer for BOM which was still quite complex and required perfect channel knowledge.

In this paper, we begin by reviewing the basics of BOM and the use of trained and decision-directed (DD) least mean squares (LMS) adaptive algorithms for equalization of BOM. Then, we address the unsuitability in using the two most popular classical blind algorithms — the Constant Modulus Algorithm (CMA) and the Shalvi-Weinstein Algorithm (SWA). Though these classical algorithms are unsuitable for BOM, it is useful to consider them in the design of new algorithms for blind equalization of BOM. Whereas the blind algorithm for BOM proposed in [1] had connections to CMA, our main contribution in this paper is a novel blind algorithm for BOM in the spirit of the Shalvi-Weinstein algorithm, and thus it relies on a spectral prewhitener before equalization. We show that the ZF solutions are stationary points of TROMBONE, and we present several numerical examples and simulations which demonstrate its performance relative to DD-LMS and the algorithm proposed in [1].

Throughout this paper, we assume all signals are real. We use $^\top$ to denote matrix transpose, $[\boldsymbol{S}]_{i,j}$ to denote the i,jth entry of the matrix $\boldsymbol{S}$, and $[\boldsymbol{S}]_i$ to denote the ith column of the matrix $\boldsymbol{S}$. The unit vector consisting of a 1 in the ith location will be denoted $\boldsymbol{e}_i$, and the function $\delta[n]$ will be the discrete Kronecker delta function.

2. BACKGROUND

2.1. Biorthogonal Modulation

An M-ary biorthogonal symbol contains $M/2$ chips, and is constructed by drawing from a set of $M/2$ orthonormal waveforms and their negatives, resulting in M possible symbols. Let $K \triangleq M/2$ and $\boldsymbol{S} \in \mathbb{R}^{K\times K}$ such that $\boldsymbol{S}^\top\boldsymbol{S} = \boldsymbol{I}$ is an orthogonal matrix whose columns comprise the basis for the biorthogonal waveforms. Since $\boldsymbol{S}$ is square, that the rows of $\boldsymbol{S}$ are also orthonormal, i.e. $\boldsymbol{S}\boldsymbol{S}^\top = \boldsymbol{I}$. We denote the symbol transmitted at time n by $\boldsymbol{x}[n]$ where $\boldsymbol{x}[n] \in \{\pm[\boldsymbol{S}]_0, \pm[\boldsymbol{S}]_1, \ldots, \pm[\boldsymbol{S}]_{K-1}\}$, and we assume all symbols are i.i.d. and equiprobable. We use a polyphase representation for the corresponding serial chip-rate process, denoting the ith chip of the nth symbol by $x[Kn-i]$, where $i \in \{0,\ldots,K-1\}$.

While the symbols are i.i.d., the chips are most certainly not. Nevertheless, the second-order statistics of the chip-rate random process are decorrelated and obey

$$E\left[x[Kn-i]x[Km-j]\right] \quad = \quad 1/K\delta[n-m]\delta[i-j]$$

which can be shown by using the fact that the symbols are i.i.d. and zero-mean, and that the rows of $\boldsymbol{S}$ are orthonormal.

2.2. System Model

The system model is shown in Fig. 1. The BOM chips $x[Kn-i]$ are transmitted through a causal linear time-invariant channel with finite impulse response $\boldsymbol{h} = [h[0], h[1], \ldots, h[N_h-1]]^\top$ and additive white Gaussian noise $w[Kn-i]$ of variance σ_w^2. The received chip stream $y[Kn-i]$ is passed through a linear equalizer with impulse response $\boldsymbol{f} = [f[0], f[1], \ldots, f[N_f-1]]$. We express the channel impulse response in matrix form by defining $\boldsymbol{\mathcal{H}} \in \mathbb{R}^{N_f\times N_c}$ as the Tœplitz channel impulse response matrix where $[\boldsymbol{\mathcal{H}}]_{i,j} = h[j-i]$. Then, the regressor matrix $\boldsymbol{Y}[n] \in \mathbb{R}^{N_f\times K}$ of received chips can be written $\boldsymbol{Y}[n] = \boldsymbol{\mathcal{H}}\boldsymbol{X}[n] + \boldsymbol{W}[n]$ where $N_c \triangleq N_f + N_h - 1$, $\boldsymbol{X}[n] \in \mathbb{R}^{N_c\times K}$ is the Hankel matrix of chips defined as

[*]Supported in part by Applied Signal Technology and NSF Grants CCF-0310023 and INT-0233127. CRJ also supported in part by a Fulbright Research Scholarship to France in 2005. Email: agk5@cornell.edu

$[\boldsymbol{X}[n]]_{i,j} = x[Kn-i-j]$, and $\boldsymbol{W}[n] \in \mathbb{R}^{N_f \times K}$ is the Hankel matrix of noise samples defined as $[\boldsymbol{W}[n]]_{i,j} = w[Kn-i-j]$. Then, the symbol output by the equalizer at time n can be written $\boldsymbol{z}[n] = \boldsymbol{Y}^\top[n]\boldsymbol{f}$.

The equalizer output is passed into the decision device, which is assumed to be the memoryless Euclidean distance detector (i.e. a correlation detector [3]). This can be implemented simply by forming the correlation $\boldsymbol{S}^\top \boldsymbol{z}[n]$, and deciding in favor of the component with largest magnitude while taking the sign into account. We have chosen this detector for its simplicity and low latency. When the equalizer is operating correctly, the decision device output is $\hat{\boldsymbol{x}}[n] \approx \boldsymbol{x}[n-\Delta]$ where Δ is the symbol delay through the combined channel and equalizer. We will also use the combined channel/equalizer response, which can be written as $\boldsymbol{c} \triangleq \boldsymbol{\mathcal{H}}^\top \boldsymbol{f}$.

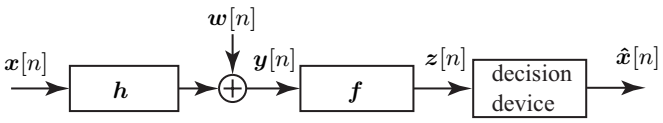

Fig. 1. System Model

3. CLASSICAL EQUALIZATION APPLIED TO BOM

3.1. MMSE and LMS Equalizers

The minimum mean squared error equalizer, a standard benchmark of equalizer performance, follows from straightforward Wiener filter theory, and was previously presented in [1] as

$$\boldsymbol{f}_{MSE} = \left(\boldsymbol{\mathcal{H}}\boldsymbol{\mathcal{H}}^\top + K\sigma_w^2 \boldsymbol{I}\right)^{-1} \boldsymbol{\mathcal{H}}\boldsymbol{e}_{K\Delta}. \quad (1)$$

Since the mean-squared error is quadratic, we can use the LMS algorithm to calculate $\boldsymbol{f}$ adaptively when training data is available. This results in the LMS update equation

$$\boldsymbol{f}_{LMS}[n+1] \quad = \quad \boldsymbol{f}_{LMS}[n] - \mu \boldsymbol{Y}[n]\left(\boldsymbol{z}[n] - \boldsymbol{x}[n-\Delta]\right)$$

where μ is a small positive step-size. The presence of $\boldsymbol{x}[n-\Delta]$ in the update term implies the availability of training data; when training data is unavailable, we can replace $\boldsymbol{x}[n-\Delta]$ with the output of the decision device, $\hat{\boldsymbol{x}}[n]$, resulting in the DD-LMS algorithm.

Decision-directed algorithms typically require an open eye initialization, and as discussed in [1] the open eye regime for BOM is in general smaller than the open eye regime for traditional BPSK. Decision directed adaptation is generally not a good choice for cold startup of BPSK equalizers, and the situation may only be worse for BOM signals. This motivates the search for blind methods of equalizer adaptation for BOM other than decision direction.

3.2. Classical Blind Approaches

When faced with the task of designing a blind adaptive equalization algorithm for a new modulation scheme, a natural path is to consider the use of classical approaches. The two most common classical algorithms are the CMA [4] and the Shalvi-Weinstein algorithm (SWA) [5]. The CMA is a dispersion minimization algorithm that requires that the source sequence to have sub-Gaussian kurtosis, since for sources with super-Gaussian kurtosis the CMA results in ISI enhancement [6]. The BOM chips can easily be shown to have super-Gaussian kurtosis, for example when $\boldsymbol{S} = \boldsymbol{I}$ and $K > 3$, and thus the CMA is not a suitable choice for equalization of BOM signals. The SWA, on the other hand, can still be used on sources with super-Gaussian kurtosis, by a simple sign change in the algorithm [5]. The SWA maximizes the magnitude of the kurtosis of the equalizer output, where the cost is $J_{SWA}(\boldsymbol{f}) = |\mathcal{C}_4(z[Kn-i])|$ with a unit-norm constraint on the equalizer taps. Note that the SWA, being a constrained algorithm, has the additional requirement that pre-whitening be performed before equalization so that the effective channel is white. The rationale for this criterion is based on the fact that, for i.i.d. sources, and when the equalizer output power is constrained to equal the power of the source process, the magnitude of the channel/equalizer output kurtosis is less than or equal to the magnitude of the source kurtosis, or $|\mathcal{C}_4(z[Kn-i])| \leq |\mathcal{C}_4(x[Kn-i])|$. Equality occurs when ISI has been eliminated, and so constrained maximization of $J_{SWA}(\boldsymbol{f})$ seems like a sensible approach. As is the case with the CMA, however, the standard analysis [5] of the SWA assumes that the source is i.i.d. The fact that the BOM chips are not i.i.d. causes the kurtosis of the BOM source to be periodically time-varying with period K. This presents a problem since some phases of the signal at the channel/equalizer output can have kurtosis less than the source signal, while other phases can be greater. This situation occurs, for example, when a BOM source with $\boldsymbol{S} = \boldsymbol{I}$ and $K = 2$ passes through the channel/equalizer $\boldsymbol{c} = [1,\ 1]^\top/\sqrt{2}$, resulting in $|\mathcal{C}_4(z[Kn-1])| < |\mathcal{C}_4(x[Kn-i])| < |\mathcal{C}_4(z[Kn])|$. This violates the fact upon which the motivation for SWA was based, and so the non-i.i.d. nature of the BOM signal also renders the SWA unsuitable as a candidate algorithm.

4. THE TROMBONE ALGORITHM

4.1. Algorithm Description

As we have discussed, the two most popular classical blind equalization algorithms are the CMA and the SWA. Since previous study of an algorithm for BOM drew largely from the spirit of the CMA [1], a sensible next step is to consider how we might apply the SWA philosophy to equalization of BOM signals.

When the channel has been appropriately equalized, the correlator output $\boldsymbol{S}^\top \boldsymbol{z}[n]$ should be a canonical unit vector (modulo sign). We observe that for any ℓ_p norm, we desire $||\boldsymbol{S}^\top \boldsymbol{z}[n]||_p = 1$. For any $p < q$ and any vector $\boldsymbol{x}$, we have $||\boldsymbol{x}||_p^m \geq ||\boldsymbol{x}||_q^m$ with equality when $\boldsymbol{x}$ is a canonical unit vector. This fact is the motivation for our algorithm, termed "TROMBONE" (for **T**he **R**ecovery **O**f M-ary **BiO**rthogonal signals via p-**N**orm **E**quivalence) and having cost function

$$J_{TRO}(\boldsymbol{f}) \quad = \quad E\left[||\boldsymbol{S}^\top \boldsymbol{z}[n]||_p^m - ||\boldsymbol{S}^\top \boldsymbol{z}[n]||_q^m\right]. \quad (2)$$

When the equalizer is operating correctly so that the correlator outputs are "perfect", the cost will be zero as hoped. We also note that the trivial solution has zero cost, so to avoid this solution we need to impose a constraint on the algorithm. Here, we choose to constrain the equalizer output power to be $E[||\boldsymbol{z}[n]||_2^2] = E[||\boldsymbol{x}[n]||_2^2]$, which amounts to $\boldsymbol{c}^\top \boldsymbol{c} = 1$ in the absence of noise. While in general we could consider any m, p, q so long as $p < q$, we focus on the case $p = 2$, $m = q = 4$. Just as the fourth-order cumulant (i.e. the kurtosis) can be defined for an i.i.d. scalar random process, cumulants can also be defined for i.i.d. vector random processes [7]. Expanding our cost in terms of cumulants, the cost becomes

$$\begin{aligned} J_{TRO}(\boldsymbol{f}) \quad &= \quad E\left[||\boldsymbol{S}^\top \boldsymbol{z}[n]||_2^4 - ||\boldsymbol{S}^\top \boldsymbol{z}[n]||_4^4\right] \quad (3) \\ &= \quad \sum_{\substack{i,j \\ i \neq j}} [\mathcal{C}_4(\boldsymbol{S}^\top \boldsymbol{z})]_{i,i,j,j} + 2\sum_{i,j}\left[\mathcal{C}_2(\boldsymbol{S}^\top \boldsymbol{z})\right]_{i,j}^2 \quad (4) \\ &\quad + \left(\sum_i \left[\mathcal{C}_2(\boldsymbol{S}^\top \boldsymbol{z})\right]_{i,i}\right)^2 - 3\sum_i \left[\mathcal{C}_2(\boldsymbol{S}^\top \boldsymbol{z})\right]_{i,i}^2 \end{aligned}$$

The constraint that we have imposed, i.e. $\boldsymbol{c}^\top \boldsymbol{c} = 1$, is a function of the combined channel/equalizer response. In practice, we do not have knowledge of $\boldsymbol{c}$. However, if we assume spectral pre-whitening has been performed before equalization as in [5], thereby assuming the effective channel is white, the constraint becomes

$$\boldsymbol{c}^\top \boldsymbol{c} = 1 \implies \boldsymbol{f}^\top \boldsymbol{\mathcal{H}} \boldsymbol{\mathcal{H}}^\top \boldsymbol{f} = \boldsymbol{f}^\top \boldsymbol{f} = 1$$

so that normalization of the equalizer taps ensures that we will meet the constraint. The instantaneous gradient gives the algorithm update equation with a normalization step as

$$\begin{aligned} \boldsymbol{f}'_{TRO}[n+1] &= \boldsymbol{f}_{TRO}[n] - \mu \boldsymbol{Y}[n] \cdot \\ &\quad \left(\boldsymbol{z}[n]^\top \boldsymbol{z}[n] \boldsymbol{I} - \boldsymbol{S}\, \mathrm{diag}(\boldsymbol{S}^\top \boldsymbol{z}[n])^2 \boldsymbol{S}^\top \right) \boldsymbol{z}[n] \\ \boldsymbol{f}_{TRO}[n+1] &= \boldsymbol{f}'_{TRO}[n+1] / \sqrt{\boldsymbol{f}'^\top_{TRO}[n+1] \boldsymbol{f}'_{TRO}[n+1]} \end{aligned}$$

where $\mathrm{diag}(\boldsymbol{x})$ is the square diagonal matrix having $\boldsymbol{x}$ along its diagonal.

We see this algorithm does appear to have some vague similarities with the SWA in that we have a constrained cost function, motivated by the fact that $||\boldsymbol{S}^\top \boldsymbol{z}[n]||_4^2 \geq ||\boldsymbol{S}^\top \boldsymbol{z}[n]||_4^4$ with equality when ISI has been eliminated. The algorithm also shares some similarity with the Shtrom-Fan algorithms [8] in that it involves a difference of two ℓ_p-norms. Beyond this similarity, however, our algorithm is fundamentally different from the Shtrom-Fan algorithms which require the data to be i.i.d. at the chip level.

We define the ZF solutions as those where the combined channel/equalizer response $\boldsymbol{c} = \boldsymbol{e}_{K\Delta}$. Note that, unlike more traditional equalization problems, our definition of the ZF solutions only includes responses with delays that are a multiple of K. In situations where the delay is not a multiple of K, the decision device will not be operating on the symbol boundary, and these points are not generally stable points of the algorithm.

We will now show that the ZF solutions are stationary points. Taking the derivative of the unconstrained TROMBONE cost function, and exploiting the linearity property of cumulants gives

$$\frac{1}{4} \frac{\partial J_{TRO}(\boldsymbol{f})}{\partial f[n]} = \sum_m h[p-n] \Lambda[m]$$

where $\Lambda[m]$ is defined on the next page in (6).

To see the that ZF solutions are stationary points of the TROMBONE cost function, we evaluate the gradient at $\boldsymbol{c} = \boldsymbol{e}_{K\Delta}$ (which, we should note, satisfies the unit-norm constraint). Indeed, after substitution, the gradient reduces to the all zero vector, and thus the ZF solutions are stationary points of the algorithm. We could equivalently use the method of Lagrange multipliers, but since the ZF solutions are stationary points and simultaneously satisfy the unit-norm constraint, the Lagrange multiplier is zero. From our observations through simulation, we believe the stationary points at the ZF solutions are also locally stable, as we have tested this claim on thousands of pre-whitened channels. Simple examination of the Hessian eigenvalues of constrained algorithms does not allow us to generically classify these stationary points as minima; we would need to resort to perturbation analysis or re-parameterization of the cost function as we will now show in a low dimensional example.

4.2. Example 1: Stationary Points in Low Dimensions

We now classify all the stationary points for a low-dimensional example. Working in the combined channel/equalizer domain $\boldsymbol{c}$, we let $\boldsymbol{S} = \boldsymbol{I}_2$ and $N_c = 3$. Because the unit norm tap constraint is difficult to apply in the $\boldsymbol{c}$ domain, we need a transform to re-parameterize the cost function in a coordinate system that permits us to easily apply the constraint. We can re-parameterize the function of $\boldsymbol{c}$ in polar coordinates, having $N_c - 1$ rotation angles $\{\theta_0, \ldots, \theta_{N_c-2}\}$ and one radius r. One possibility [6] for parameterizing $\boldsymbol{c}$ in polar form is to choose

$$c[n] = \begin{cases} r \sin(\theta_n) \prod_{j=0}^{n-1} \cos(\theta_j) & 0 \leq n \leq N_c - 2 \\ r \cos(\theta_{N_c-1}) \prod_{j=0}^{N_c-2} \cos(\theta_j) & n = N_c - 1 \end{cases} \quad (5)$$

so that by fixing $r = 1$, any arbitrary unit-norm $\boldsymbol{c}$ may be reached for an essentially unique choice of rotation angles.

Substituting (5) into the TROMBONE cost function with $\boldsymbol{S} = \boldsymbol{I}_2$, setting the gradient to zero, and zeroing all but $N_c = 3$ taps results in a system of equations in two parameters, θ_0 and θ_1. We can solve for the locations of all stationary points exactly, and they have been tabulated in Table 1. For this particular example, we see that the only minima of the TROMBONE cost surface are the ZF solutions. There are not minima at $\boldsymbol{c} = \pm[0, 1, 0]^\top$, and this point was specifically excluded in our definition of ZF solutions since the delay is not a multiple of K; however, this point corresponds to a degenerate saddle point, which implies the cost surface is very flat, and the adaptive algorithm may suffer convergence speed problems as it passes through this region.

Table 1. TROMBONE Stationary Points for Example 1

$\boldsymbol{c}^\top$	type
$\pm[1, 0, 0], \pm[0, 0, 1]$	minima
$\pm[\sqrt{1/2},\ 0,\ -\sqrt{1/2}], \pm[\sqrt{1/2},\ 0,\ \sqrt{1/2}]$	saddle points
$\pm[0,\ 1,\ 0]$	deg. saddle pts

4.3. Example 2: False Minima of TROMBONE

While Example 1 provides some hope of convergence to solutions with globally optimal performance, we now investigate stationary points that arise in impulse responses with larger lengths of contiguous non-zero taps. We conducted a (non-exhaustive) numerical search for stationary points with larger channel/equalizer lengths, while maintaining $\boldsymbol{S} = \boldsymbol{I}_2$. The ZF solutions are of course minima in this situation, but we do observe the presence of additional local minima once the number of non-zero taps grows to $N_c \geq 6$.

Through experimentation (and analytic confirmation) we found a class of stationary points with impulse response of the form $\boldsymbol{c}^* = \pm[0,\ \alpha,\ \beta,\ \gamma,\ -\beta\,, \alpha]^\top$, for $\alpha \approx 0.2973, \beta \approx 0.5425, \gamma \approx 0.4844$, which was found to be a minimum by analysis of the re-parameterized Hessian. As N_c is increased beyond 6, this minimum persists in higher dimensions. And, any $K = 2$ tap shift of this impulse response is also a local minimum (i.e. any response obtained by adding an even number of zeros to the front).

5. NUMERICAL EXAMPLES

5.1. Visualizing the TROMBONE Cost Surface

Considering the noiseless case with $\boldsymbol{S} = \boldsymbol{I}_2$ and $N_c = 2$, we have plotted a 2-D slice of the unconstrained TROMBONE cost surface in Fig. 2a. The unit norm constraint will force the algorithm to stay on contour indicated by the dotted circle in these two dimensions. For the case of $\boldsymbol{S} = \boldsymbol{I}$, the cost surface is a single trough with a bulb at the origin, and the cost is zero along the $c[0]$ axis.

Identifying the stationary points from the unconstrained cost, however, is not easy. Thus, similar to what was done in Section 4.2,

$$\Lambda[m] = \sum_{i_1,i_2,i_3,i_4} [\mathcal{C}_4(\boldsymbol{x})]_{i_1,i_2,i_3,i_4} \sum_{k_1,k_2} \sum_p \delta[Kp+i_1-k_1-m]c[Kp+i_2-k_1]c[Kp+i_3-k_2]c[Kp+i_4-k_2] \quad (6)$$

$$- \sum_{i_1,i_2,i_3,i_4} [\mathcal{C}_4(\boldsymbol{x})]_{i_1,i_2,i_3,i_4} \sum_{k_1,k_2,k_3,k_4} \sum_j \left[[\boldsymbol{S}]_{k_1,j}[\boldsymbol{S}]_{k_2,j}[\boldsymbol{S}]_{k_3,j}[\boldsymbol{S}]_{k_4,j} \sum_p \delta[Kp+i_1-k_1-m]c[Kp+i_2-k_2]c[Kp+i_3-k_3]c[Kp+i_4-k_4] \right]$$

$$- \frac{3}{K^2} \sum_{i_1,i_2,i_3,i_4} \sum_j [\boldsymbol{S}]_{i_1,j}[\boldsymbol{S}]_{i_2,j}[\boldsymbol{S}]_{i_3,j}[\boldsymbol{S}]_{i_4,j} \sum_p c[m+i_1-i_2]c[p-i_3]c[p-i_4] + \frac{2}{K^2} \sum_p \sum_{k_1,k_2} c[m+k_1-k_2]c[p-k_1]c[p-k_2] + c[m] \left(\sum_p c^2[p] \right)$$

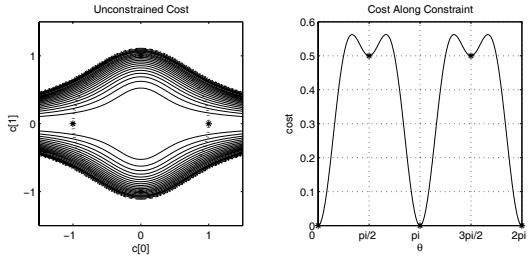

Fig. 2. TROMBONE Cost Surface for $\boldsymbol{S} = \boldsymbol{I}$

we transform the 2-parameter cost plot into polar coordinates with a single rotation angle. Looking at the cost function in polar coordinates, where the angle $\theta = \tan^{-1}(c[1]/c[0])$, we can more easily see the stationary points as shown in Fig. 2b. There are minima at the ZF solutions, as well as minima at $\boldsymbol{c} = \pm[0,1]^\top$, though this latter minimum is quite shallow. Stationary points of low-dimensional slices may change their character in higher dimensions; we know from Example 1 that the stationary point at $\boldsymbol{c} = \pm[0,1]^\top$ becomes a degenerate stationary point in higher dimensions.

5.2. Simulation Near Zero-Forcing Solutions

To provide verification that our analysis of the local behavior of our algorithm is valid, we consider a simulation where we initialize the algorithm in a ball around a ZF solution, and observe the ability of the algorithm to converge as the ball radius is increased. We operate in a noiseless scenario, a channel with response $\boldsymbol{h} = [-0.4, 0.84, 0.336, 0.1344, 0.0538, 0.0215]^\top$, we have chosen $N_f = 30$ equalizer taps, and we choose the signal bases $\boldsymbol{S} = \boldsymbol{I}_2$. Note that the channel is approximately white (i.e. $\boldsymbol{\mathcal{H}}\boldsymbol{\mathcal{H}}^\top \approx \boldsymbol{I}$), and the corresponding ZF equalizer satisfies $\boldsymbol{f}_{ZF}^\top \boldsymbol{f}_{ZF} = 1$.

As initializations, we chose 1,000 points uniformly distributed in a ball around the ZF solution, and we observed the ability of the algorithms to converge to a ZF solution as the radius of the ball increased. We ran the algorithms for 10,000 symbols at each of the 1,000 initializations, and declared the algorithm to have converged if the MSE was less than 10^{-3}. As shown in Fig. 3, all of the algorithms converge to the ZF solution when the size of the ball of initializations around the ZF solution is less than 1, thus verifying our analysis of local convergence. For larger radii beyond 1, which we can hardly consider to be "local" to the ZF solutions, we see that all algorithms still converge with a fairly high percentage, though possibly to a ZF solution corresponding to another delay. Furthermore, the blind algorithms both outperform DD-LMS. The curves are all monotone non-increasing, albeit with some jumps due to the nonlinear nature of the cost surfaces, and for large radii the convergence percentages eventually reach a constant value. This is because, beyond a sufficiently large initialization ball radius, there is no notion of locality; the ball grows to encompass the entire space, and so increasing the radius further has no effect on convergence percentage.

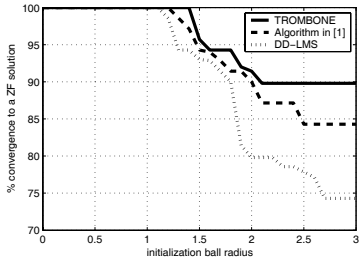

Fig. 3. Convergence percentage vs. initialization distance from ZF solution

5.3. Conclusion

While energy efficient modulations are being given serious attention by industry for use in environments with ISI, little attention has been given to equalization of such signals. Due to the non-i.i.d. nature of these signals, direct application of classical equalization techniques is not possible. We have attempted to address this difficulty, and have proposed a novel blind algorithm for the equalization of BOM signals. We then addressed the local convergence of this algorithm, and demonstrated its performance.

6. REFERENCES

[1] A.G. Klein, C. R. Johnson, Jr., and P. Duhamel, "On blind equalization of M-ary bi-orthogonal signaling," in *Proc. IEEE Intl. Conf. on Acoustics, Speech, and Signal Processing (ICASSP'05)*, Mar. 2005.

[2] K. Takizawa and R. Kohno, "Low-complexity RAKE reception and equalization for MBOK DS-UWB systems," in *GLOBECOM'04*, Nov. 2004, vol. 2, pp. 1249–1253.

[3] J.G. Proakis, *Digital Communications*, McGraw-Hill, New York, 4 edition, 2000.

[4] D. N. Godard, "Self-recovering equalization and carrier tracking in two-dimensional data communication systems," *IEEE Trans. Commun.*, vol. 28, pp. 1867–1875, Nov. 1980.

[5] O. Shalvi and E. Weinstein, "New criteria for blind deconvolution of nonminimum phase systems (channels)," *IEEE Trans. Inform. Theory*, vol. 36, pp. 312–321, Mar. 1990.

[6] P. A. Regalia, "On the equivalence between the godard and shalvi-weinstein schemes of blind equalization," *Signal Processing (Elsevier)*, vol. 73, pp. 185–190, Feb. 1999.

[7] Lieven De Lathauwer, *Signal Processing based on Multilinear Algebra*, Ph.D. thesis, Katholieke Universiteit Leuven, Leuven, Belgium, Sept. 1997.

[8] V. Shtrom and H. Fan, "New class of zero-forcing cost functions in blind equalization," *IEEE Trans. Signal Processing*, vol. 46, pp. 2674–2683, Oct. 1998.